Received: 11 September 2021 | Revised: 19 December 2021 | Accepted: 6 January 2022

DOI: 10.1002/mgg3.1878

Molecular Genetics & Genomic Medicine Open Access WILEY

ORIGINAL ARTICLE

Genetic and functional analyses detect an *EXT1* splicing pathogenic variant in a Chinese hereditary multiple exostosis (HME) family

Jianwei Li[1] | **Zhiqiang Wang**[2] | **Yaxin Han**[3] | **Chengfang Jin**[2] | **Dalin Cheng**[2] | **Yong-An Zhou**[1] | **Junping Zhen**[1]

[1]The Second Hospital, Shanxi Medical University, Taiyuan, China

[2]Lvliang People's Hospital, Shanxi Medical University, Lvliang, China

[3]The First Hospital, Shanxi Medical University, Taiyuan, China

Correspondence
Yong-An Zhou and Junping Zhen, The Second Hospital, Shanxi Medical University, Taiyuan, China.
Email: zya655903@163.com and doctorzjp@sxmu.edu.cn

Funding information
National Natural Science Foundation of China, Grant/Award Number: 82172011

Abstract

Background: Hereditary multiple exostosis (HME) is an autosomal dominant skeletal disorder characterized by the development of multiple cartilage-covered tumors on the external surfaces of bones (osteochondromas). Most of HME cases result from heterozygous loss-of-function mutations in *EXT1* or *EXT2* gene.

Methods: Clinical examination was performed to diagnose the patients: Whole exome sequencing (WES) was used to identify pathogenic mutations in the proband, which is confirmed by Sanger sequencing and co-segregation analysis: qRT-PCR was performed to identify the mRNA expression level of *EXT1* in patient peripheral blood samples: minigene splicing assay was performed to mimic the splicing process of *EXT1* variants in vitro.

Results: We evaluated the pathogenicity of *EXT1* c.1056 + 1G > T in a Chinese family with HME. The clinical, phenotypic, and genetic characterization of patients in this family were described. The variant was detected by whole-exome sequencing (WES) and confirmed by Sanger sequencing. Sequencing of the RT-PCR products from the patient's blood sample identified a large deletion (94 nucleotides), which is the whole exome 2 of the *EXT1* cDNA. Splicing assay indicated that the mutated minigene produced alternatively spliced transcripts, which cause a frameshift resulting in an early termination of protein expression.

Conclusions: Our study establishes the pathogenesis of the splicing mutation *EXT1* c.1056 + 1G > T to HME and provides scientific foundation for accurate diagnosis and precise medical intervention for HME.

KEYWORDS

c.1056 + 1G > T, *EXT1*, hereditary multiple exostosis, splicing variant, whole exome sequencing

Jianwei Li and Zhiqiang Wang contributed equally as first author.

1 | INTRODUCTION

Hereditary multiple exostoses (HME), also called hereditary multiple osteochondromas, is a rare genetic disorder that causes the development of multiple cartilage-covered tumors on the external surfaces of bones (osteochondromas) and inherited in an autosomal dominant manner with a prevalence of 1:50,000 in Western countries (D'Arienzo et al., 2019). More than 90% of HME cases result from heterozygous loss-of-function mutations in *EXT1* (OMIM #608177) or *EXT2* (OMIM #608210) gene (Pacifici, 2017). Most of the patients are asymptomatic at birth; thus, genetic screenings are the only proven diagnostic method currently used for the newborns of affected families (Schmale et al., 1994). After 3 years old, some palpable masses were found near the joints. Knees, shoulders, ankles, and wrists are the most involved joints (Hennekam, 1991), and they can be easily diagnosed with imaging examination (X-ray, CT, MRI).

The *EXT1* gene is located on the long arm of human chromosome 8 (8q24.11), and the *EXT2* gene is located on the short arm of human chromosome 11 (11p11.2). They encode exostosin 1 (EXT1) and exostosin 2 (EXT2), respectively. Both proteins are localized at the Golgi apparatus, forming a rather stable complex that is responsible for the synthesis and assembly of heparan sulfate (HS) chains onto the core protein of syndecans, glypicans, and other HS-rich proteoglycans (McCormick et al., 2000). Research shows that heparan sulfate proteoglycans (HSPGs), composed of core protein and heparan sulfate (HS) chains, are involved in a wide range of developmental and physiological functions in the extracellular matrix (ECM) and on the cell surface. The most important interaction occurs between them and key signaling proteins (e.g., the fibroblast growth factor (FGF), bone morphogenetic protein (BMP), hedgehog families, etc.), which regulates protein diffusion, distribution, turnover, and action on target cells and tissues. (Billings & Pacifici, 2015).

Heterozygous mutations of either EXT gene may cause HME. Among them, the HME requires bi-allelic mutations that would affect local cells, which would be unable to retain a normal phenotype, and turn them into tumorigenic cells. This has been confirmed in the majority of patients (nearly 75%) with HME who were found to harbor *EXT1* mutations. However, it has been reported that haploinsufficiency appears to be insufficient to trigger osteochondroma formation (Huegel et al., 2013). According to the Knudson two-hit hypothesis (Knudson, 1971), osteochondroma formation was reported in animal models and was also reported in several patients with HME (Zak et al., 2011).

As documented in the Human Gene Mutation Database (http://www.hgmd.cf.ac.uk), 567 mutations in *EXT1* and 281 mutations in *EXT2* have been reported until now, involving 34.1% point mutation (including nonsense and missense mutation), 10.8% splice mutation, and 55.1% structural variation (including copy number variation, translocation, and inversion). Splicing mutations currently account for a small fraction of the *EXT* mutational spectrum, but the proportion is probably underestimated due to the conventional splice mutation screening strategies. Here, we identified an *EXT1* (OMIM #608177, Genbank reference sequences: NM_000127.2) splicing pathogenic variant c.1056 + 1G > T that causes abnormal splicing in a three-generation Chinese family with HME. In the present paper, we aimed to characterize the molecular effect and mechanism of the *EXT1* GT-AG intron pathogenic variant that causes HME.

2 | MATERIAL AND METHODS

2.1 | Study participants

In this study, a Chinese family with HME including 13 people in three generations were admitted to the hospital(Figure 1a). All patients in this family participated in the present study and agreed to publication. The unaffected members of the family were taken as a control group. We can distinguish HME from non-HME patients based on clinical manifestations and physical examinations, including X-ray, computed tomography, and MRI. Some people in this family had accepted blood routine examination and lipid profile test. The concentrations of serum lipids included were high density liptein cholesterol (HDL-C), low density liptein cholesterol (LDL-C), total cholesterol (TC), and triglyceride (TG). All the participants had signed informed consents.

2.2 | Whole exome sequencing (WES) and variant confirmation

Whole exome sequencing was conducted by Aegicare (Shenzhen, China), the genomic DNA was isolated from the peripheral blood of the proband (III-8). Library preparation and sequencing were performed using Agilent SureSelect v6 reagents (Agilent Technologies, Santa Clara, CA, United States) and Illumina HiSeq 2500 (Illumina, San Diego, CA, United States). The read length at the end of the pair reaches 150 bp by using the Covaris S2 ultrasonoscope (Applied Biosystems, USA), and the sequencing depth of the capture region is approximately 100×, as sequencing also covered the intron-exon junction. The human genome reference sequence (GRCh37/hg19) was used to map the sequence reads. Based on public databases

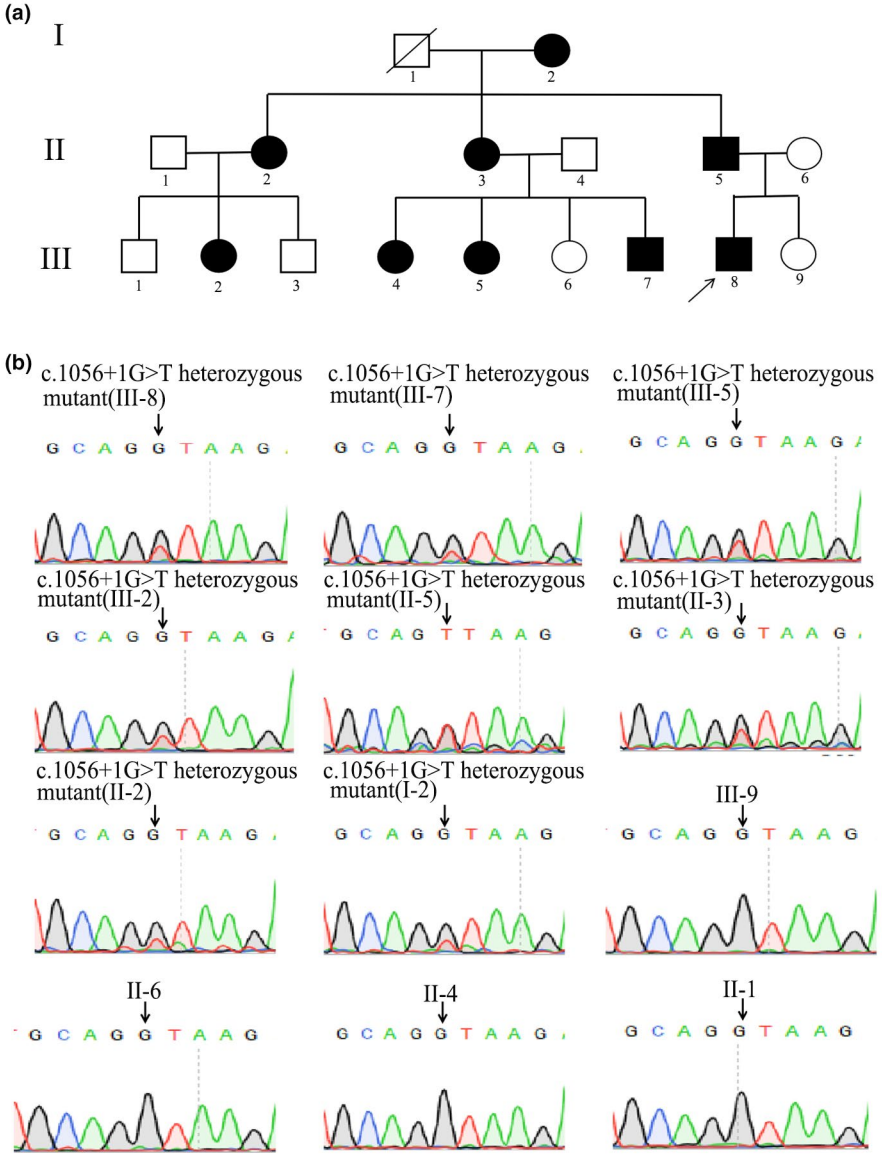

FIGURE 1 Pedigree and sequencing of this family (a) The pedigree of the family. Affected individuals are indicated by filled black, the proband is pointed by an arrow. (b) Sanger sequencing analysis performed on the genome DNA from this family. The variant was labeled by black arrow

of normal human variation (1000 g, ExAC, and gnomAD), all the variants of whose Minor Allele Frequency (MAF) was higher than 1% were filtered. American College of Medical Genetics and Genomics (ACMG) guidelines were used to interpret and classify the variants. Sanger sequencing was carried out to confirm the putatively pathogenic variants.

2.3 | Sequencing analysis

The coding region and exon-intron splice junctions including the variant of *EXT1* were analyzed using PCR amplification in combination with Sanger sequencing using the primers (Fw:5′-AGCAAAGACTGGGCAAACCA-3′; Rv:5′-AGGGAAAGTGTAGGGCTGCT-3′). The length of the product is 697 bp including intron 1, exon 2, and intron 2. Genomic DNA was extracted from peripheral blood samples, and PCR products were purified. These methods were described previously (Li et al., 2019).

2.4 | Bioinformatics analysis and prediction

Several web-based programs with different algorithms were used to analyze the potential effect of mutations on exon splicing. Genomic Evolutionary Rate Profiling

(GERP++) is a score used to calculate the conservation of each nucleotide in multispecies alignment (Davydov et al., 2010). DANN is a pathogenicity scoring methodology, and it is based on deep neural networks. The value range is 0 to 1, with 1 given to the variants predicted to be the most damaging (Quang et al., 2015). dbscSNV is a database of precomputed prediction scores for all possible SNVs that may occur in splice consensus regions, indicating whether each variant is expected to affect the splicing of the gene. There are two scores given for each variant predicted by dbscSNV, called "Ada" and "RF" scores (Jian et al., 2014). Modular Modeling of Splicing (MMSplice), a neural network scoring exon, intron, and splice sites, trained on distinct large-scale genomics datasets, predicts effects of variants on exon skipping, splice site choice, splicing efficiency, and pathogenicity (Cheng et al., 2019). SPIDEX is a computational model that uses the Percentage of Spliced-In (PSI) metric to evaluate whether a certain splicing isoform is more enriched under the presence/absence of a given variant (Xiong et al., 2015).

2.5 | Cell culture

HEK293T cells were grown in DMEM supplemented with 10% (v/v) FBS, 100 U/mL penicillin, and 100 mg/mL streptomycin at 37°C and 5% CO_2. Transfection was performed using the Polyetherimide (PEI) (PolyScience, Cat.No. 23966-2) according to the manufacturer's instructions. Transfected cells were incubated for 24 h to 48 h post-transfection.

2.6 | The minigene constructs and Western blotting

Minigene constructs including exon 2, intron 2, and exon 3 were amplified using the primer pair of *EXT1* E2-in2-E3 Fw: 5′-CCGCTCGAGCGGGAAATGCTGCACAATGC-3′ and E2-in2-E3 Rv: 5′-CCGGAATTCAACTCCCATCCATTGCTGAGCA-3′. The amplified minigene products were cloned into pEGFP-C3 cloning vector at the Xho I and EcoR I sites. The complete sequences of the minigene constructs were validated by Sanger sequencing. Minigene constructs were transiently transfected in HEK293T cells with polyetherimide (PEI) (PolyScience, Cat.No. 23966-2), and RT-PCR was performed with the same primers. RT-PCR products were separated by electrophoresis analysis and isoforms were identified by Sanger sequencing. Besides, we used Western blotting to analyze the proteins of minigene. These methods were described previously (Li et al., 2019).

2.7 | RT-PCR and qRT-PCR analysis

To evaluate the transcript variants of *EXT1* by RT-PCR in the blood cells from patients and healthy relatives, total RNA was extracted with the TRIzol following the instructions of the supplier Invitrogen, Cat. No. 15596-018). First-strand cDNA synthesis was performed using the M-MLV reverse transcriptase RNase H Minus-kit from Promega. The primer pair for RT-PCR of *EXT1* were used: Fw: 5′-TGACAGGGATAGGATCAGACAC-3′ and Rv:5′-TGTAATAACAATCTCTCATCGCCTA-3′. The primer pair for qRT-PCR of *EXT1* were used: Fw: 5′-GGGGAGAAAATCGCCGAAAGT-3′ and Rv: 5′-CATACTGAGGTGACAACTGGTC-3′. For normalization, the expression of GAPDH(Forward:CGGAGTCAACGGATTTGGTCGTAT; Reverse: AGCCTTCTCCATGGTGGTGAAGAC) was used.

3 | RESULTS

3.1 | Clinical data of the family with HME

Imaging results from different patients were marked by different phenotypes. Patients' clinical characteristics are summarized in Table 1. Specifically, out of nine patients, osteochondroma/exostoses generally occurred in the long bones of the upper and lower limbs (100% [9/9]), whereas scapulae osteochondroma/exostoses were found only in a single patient. In addition to these findings, no other suspicious affected sites were observed. About one-third (9–3/9) of patients had a deformity of the limbs and joints, and while all male patients had pain in one or more affected locations. Compared with all the patients' CT images, we found that the extent of male patients was greater than that of female patients with HME. Some aspects of the clinical features are also shown in Figure 2. To further understand the metabolic differences between patients and controls, serum lipid levels were examined in 5 patients and were shown in Table 2.

3.2 | Mutation screening and genetic analysis

We performed whole exome sequencing (WES) analysis on the proband (III-8). After filtering, we identified one splicing mutation c.1056 + 1G > T (chr8:118849346 G > T in hg19) in *EXT1* (OMIM #608177, Genbank reference sequences: NM_000127.2). The presence of the identified variant was confirmed by Sanger sequencing in the proband (III-8) and in other patients (I-2, II-2, II-3, II-5, III-2, III-4, III-5, III-7, III-8) in this family, while the

TABLE 1 Clinical characteristics of the multiple osteochondromas patients in this family

Patient	Sex	Age (years)	Age of onset, years	Location of exostoses	Surgical therapy	Pain
I-2	Female	69	Unknown	Femur, tibia, fibula	No	No
II-2	Female	47	4	Femur, tibia, fibula, knuckle	No	No
II-3	Female	43	5	Femur, tibia, fibula, humerus, phalanges	No	No
II-5	Male	37	6	Femur, tibia, fibula, humerus, ulna, scapula	No	Yes
III-2	Female	27	4	Femur, tibia, fibula	Yes	No
III-4	Female	20	3	Femur, tibia, fibula, radius, radiocarpal joint, ankle joint	No	No
III-5	Female	18	3	Femur, tibia, fibula, ulna, knuckle	No	No
III-7	Male	13	4	Femur, tibia, fibula, ulna, knuckle, radiocarpal joint, ankle joint	No	Yes
III-8	Male	7	3	Femur, tibia, fibula, humerus	No	Yes

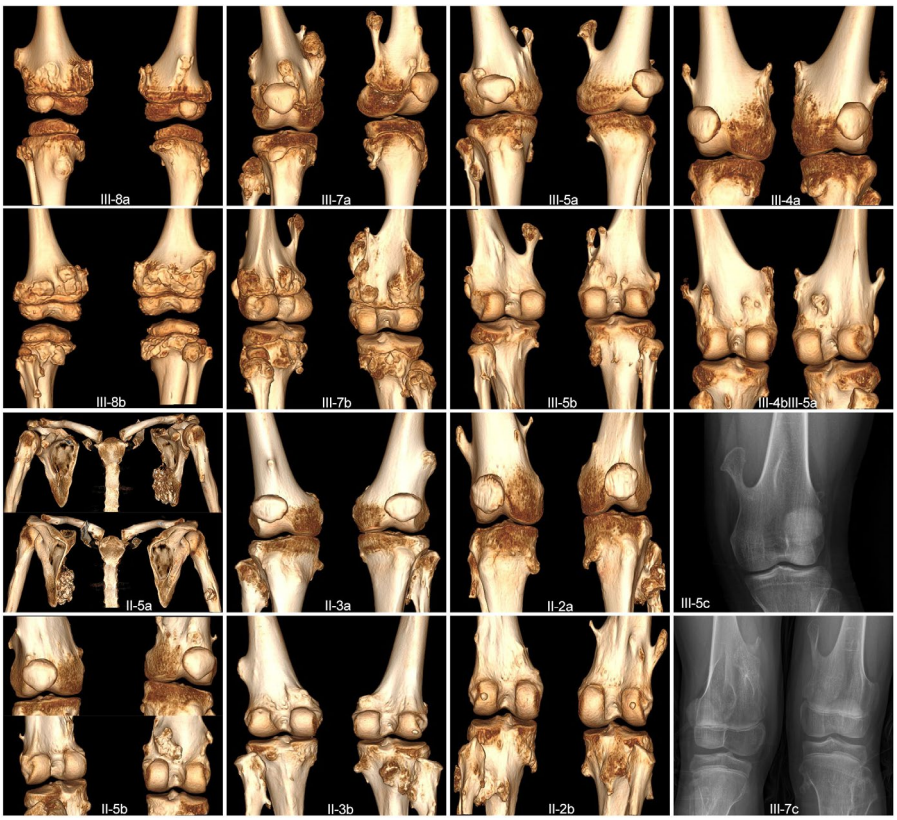

FIGURE 2 CT images and X-ray of patients show multiple lesions in the knee joint, growing away from the joint, visible bone protrusions, and cartilage caps, different patients, the length of the bone protrusions are different. One patient (II-5a) showed multiple lesions on the right scapula, and the lesions fused into a lesion. These lesions can also accumulate other bones. III-5c and III-7C is X-ray results, and the other pictures are CT image results

unaffected members of the family (II-1, II-4, II-6, III-1, III-3, III-6, III-9) did not have it (Figure 1b). Thus, the variant co-segregated with the disease in the pedigree.

This variant was not annotated in the major databases, such as the dbSNP (http://www.ncbi.nlm.nih.gov/SNP/), 1000 genome dataset (http://browser.1000genomes.org/), gnomAD (http://gnomad.broadinstitute.org), and Human Genetic Variation Browser databases (http://www.genome.med.kyoto-u.ac.jp/SnpDB/). The results describing the c.1056 + 1G > T variant were consistent with all five prediction tools (GERP++, DANN, dbscSNV, MMSplice, SPIDEX) (Table 3), as having a

detrimental effect. All three splice site prediction programs (dbscSNV, MMSplice, SPIDEX) showed that this sequence alteration abolishes the canonical splice donor site and therefore is likely to disturb normal splicing. This variant was submitted to ClinVar (https://www.ncbi.nlm.nih.gov/clinvar/RCV000255186/) with ClinVar accession code RCV000255186.

Based on these data, we classified the variant as "Pathogenic" (PVS1 + PM2 + PP1_S + PP4) according to ACMG/AMP guidelines (Richards et al., 2015).

3.3 | Splicing defect in *EXT1* c.1056 + 1G > T

The transcriptional consequence of the splice site mutation (c.1056 + 1G > T) was confirmed by the analysis of the mRNA extracted from the patient's blood. RT-PCR for the mentioned region that includes exons 1 to 3 was performed. Two bands were visualized on gel electrophoresis, 349 bp fragment, the expected wild type and 255 bp, a small fragment (Figure 3a), suggesting that the abnormal DNA fragment was generated by unique splicing events within the *EXT1* gene. The sequencing of the RT-PCR product revealed a 94-nucleotide (nt) deletion, which is the whole exome 2 of the *EXT1* cDNA (Figure 3b).

To determine whether disease progression expression levels were correlated with mRNA abundance, we performed qRT-PCR analysis. Total RNA was isolated from the blood samples of patients (III-8, III-7, II-3, II-5, I-2) and three healthy volunteers, and qRT-PCR was normalized to that of GAPDH. These results indicate that the level of *EXT1* mRNA was reduced to roughly half in the samples from adult HME patients compared to those in control. Furthermore, the expression levels in child HME patients tended to be even lower, nearly a quarter, compared to those of the control (Figure 3c). The results show that the disease progression of HME may be related to the expression level of *EXT1*. The expression level in child HME patients at the progression phase of disease was lower than the expression level in adult HME patients, which stabilized at that stage of the disease.

3.4 | Alternative splicing in minigene splicing assay

To further investigate the pathogenic mechanism of the splice site mutation (*EXT1* c.1056 + 1G > T), we constructed a minigene containing part of exon 2, exon 3, and entire intron 2 with G or T at c.1056 + 1 of *EXT1*. After transfecting HEK293T cells with the indicated vectors, total RNA was isolated, and RT-PCR was performed.

TABLE 2 The serum lipid levels of patients

Patient	Sex	Age (years)	HDL-C (ref:1.16–1.42 mmol/L)	LDL-C (ref:2.29–3.37 mmol/L)	TC (ref:2.33–5.69 mmol/L)	TG (ref:0.56–1.70 mmol/L)
I-2	Female	69	1.43↑	3.22	5.56	0.83
II-3	Female	43	1.36	2.36	4.28	1.48
II-5	Male	37	1.54↑	2.57	4.98	1.05
III-7	Male	13	1.06↓	1.29↓	2.78	0.82
III-8	Male	7	1.04↓	1.97↓	3.83	1.41

RT-PCR products were analyzed by agarose gel electrophoresis and were revealed with ethidium bromide stain. The isoforms were identified by Sanger sequencing. In both untransfected and pEGFP-*EXT1*-WT transfected HEK293T cells, clear bands of the same size were shown, which was identified as exon 2 + exon 3. But five abnormal bands were detected in mutant minigene transfected cells, and no normal bands were observed. The c.1056 + 1G > T substitution disrupts an intronic splice acceptor site, resulting in two novel 5′ splice donor sites showing up, in which sizes varied from 54 bp and 98 bp get inserted, respectively. The largest aberrant transcript inserted the entire intron 2 (Figure 4a). According to in vitro experiments, the splice variant that we demonstrated was validated as having effects on splicing, and no normally spliced transcripts were produced. The largest aberrant transcript inserted the entire intron 2 in minigene splicing assay corresponding to the transcript deletion of the whole exome 2 of the *EXT1* cDNA in the patients' blood. However, we did not find the other aberrant transcripts in the blood of the patients.

TABLE 3 Bioinformatics prediction of variant (*EXT1* c.1056 + 1G > T)

Software	Score	Cutoff
DANN	0.9957	
GERP	5.55	
dbSNV_ADA	1.000	>0.8
dbSNV_RF	0.938	>0.8
MMSplice_delta_logit_psi	−6.936	<1.5/>1.5
MMSplice_pathogenicity	1.000	≤1.5/>1.5
Spidex-Zscore	−3.542	≤2/>2

Western blot analysis of minigenes was performed to investigate the protein expression. In pEGFP-C3 vector-transfected HEK293T cells, a strong band was observed with the molecular weight of about 27 kD, which represents the GFP protein alone. In pEGFP-*EXT1*-minigene wild-type transfected cells, a band with a molecular weight at ~31 kD was observed, which was identified as the protein products of exon 2 + exon 3 fusion with GFP. However, in mutant *EXT1* minigene transfected cells, one extra band at ~32 kD molecular weight was shown compared to wild type *EXT1* minigene transfected cells, suggesting that the c.1056 + 1G > T substitution caused all frameshifts resulting in early termination of protein

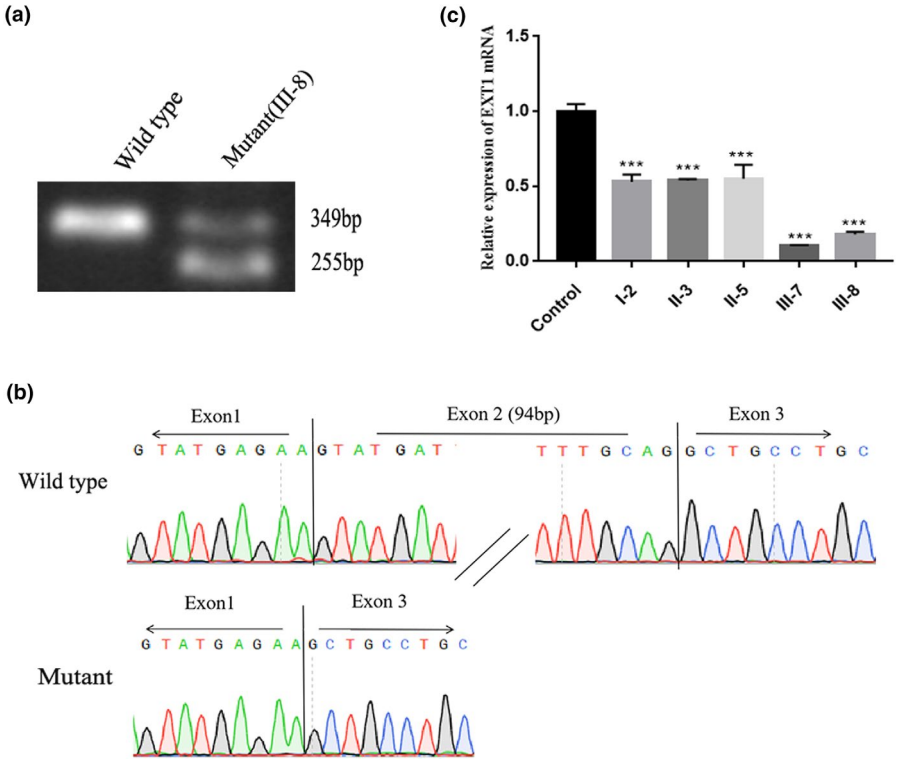

FIGURE 3 Alternative splicing of EXT1 (c.1056+1G>T). (a) mRNA from the patient blood was extracted and amplified by RT-PCR for alternative splicing of EXT1 (c.1056+1G>T). RT-PCR of the region that includes exons 1, exon2 and exon3 was performed and the PCR products were separated by gel electrophoresis. (b) Sanger sequencing analysis for the alternative splicing products. The sequence of the lower band reveals a 94-nucleotide (nt) of exon2 skiping of the EXT1 cDNA compared to wild type. (c) qRT-PCR analysis performed on total RNA obtained from blood samples of patients (I-2, II-3, II-5, III-7, III-8) and three healthy volunteers individuals. Levels were normalized to the amount of GAPDH. Data represent the mean ± *SE* of three independent measurements performed in triplicate (***$p < .001$)

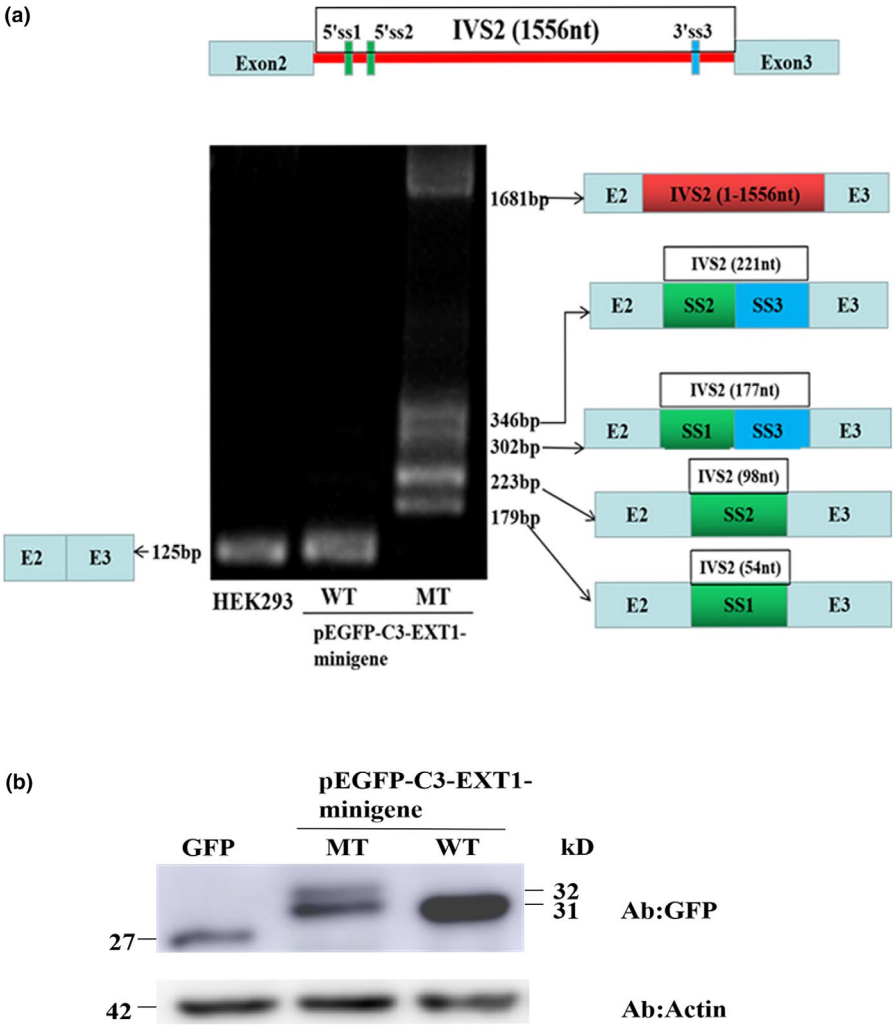

FIGURE 4 Minigene constructs for splicing pattern investigation. (a) Minigene splicing assay. EXT1 minigenes harboring the wild type or mutant EXT1 pseudoexon were transiently transfected into HEK293T cells. After RNA isolation the splicing products were analyzed by RT-PCR. (b) Western blot analysis for the expression of the wild type and mutant pEGFP-EXT1-minigenes. Whole cell lysates were separated by SDS–PAGE (12% acrylamide). GFP monoclonal antibodies were used

expression, which is consistent with the results of alternative transcript analysis (Figure 4a).

4 | DISCUSSION

The present study reported a heterozygous splice mutation (c.1056 + 1G > T) of the *EXT1* gene identified in a three-generation family with HME. Since the first identification by Wells (1997), the variation we report have been observed in populations of different ancestry. But, in fact, very few studies have focused on the pathogenicity of the variation and associated functional change. The results of this study complement and extend the underlying pathogenic mechanisms on this variation. According to the ACMG guideline, we found the mutation of c.1056 + 1G > T in *EXT1* was pathogenic (PVS1 + PM2 + PP1_S + PP4). Through the minigene analysis, two new 5′ splice-site recognition and a new 3′ splice-site recognition was identified in the MT minigene model and formed 4 different spliced products. Practically, only one abnormal transcript was detected in the patient's blood samples, which correspond to the transcript NO.5 in the minigene experiments. This may be because the minigene vectors disrupted exonic splicing enhancers, or other splicing factors are involved in regulation, which caused the results of in vitro experiments did not adequately represent the real situation in vivo.

Alternative pre-mRNA splicing is a key mechanism for increasing proteomic diversity and modulating gene expression, and splice sites (5′ and 3′), the branch site, and the polypyrimidine sequence are the key splicing signals, which play major roles in the splicing. If mutations occur

in these sites, the effective splicing of exons may be affected, which may interfere with subsequent transcription and translation (Barash et al., 2010; Wang & Cooper, 2007). The mutation identified in the present study was located at the 5′ splice site of *EXT1* intron 2, and inactivate the donor splice site, thereby generating new transcripts, or giving rise to aberrant mRNA transcripts. This aberrant transcript lacks the entire coding sequence for exon 2 (94 bp) that would cause a frameshift leading to a premature stop codon and therefore a premature termination of mRNA. The exon-skipping event, downstream premature termination codon (PTC), may initiate the nonsense-mediated mRNA decay (NMD) process, suggesting that the patient's clinical presentation may be relevant to haploinsufficiency mechanism. However, our RT–qPCR results do not fully support this assumption. The expression levels of *EXT1* mRNA in patients were reduced (probably half or less) compared with normal controls. What warrants proper attention, however, is a possible relationship between age and the expression levels of *EXT1* mRNA. The expression levels in adult HME patients are half of the normal value but those determined in child HME patients are lower than adults ad are approximately a quarter of the normal value. Lower expression levels were associated with more cartilaginous exostoses numbers and locations in child HME patients. This result may be contrary to the haploinsufficiency theory.

Human and mouse studies carried out so far have established that single heterozygous mutations in *EXT1* or *EXT2* (and the resulting 50% reduction in systemic HS levels) are not sufficient to trigger a full-fledged HME phenotype (Hecht et al., 2005). Jones et al. (2010) have also rejected the haploinsufficiency model with distinct experimentation and tend to explain HME pathogenesis according to a "second hit" theory. Reijnders et al. (2010) said that they found a second hit in 63% of analyzed osteochondromas, and the detection of the second hit may depend on the ratio of HS-positive (normal) versus HS-negative (mutated) cells in the cartilaginous cap of the osteochondroma. However, his data are combined from immunohistochemistry experiments instead of gene sequencing. Several studies have demonstrated that homozygous $EXT1^{-/-}$ mutant mice could not survive beyond 24 h of birth. Moreover, culturing of $EXT1^{-/-}$ cartilaginous cap cells failed. We are reasonably confident that homozygous $EXT1^{-/-}$ mutant cells maybe could not exist in vivo, or the mutations that occur immediately initiated apoptosis. Some studies in mice have shown that compound heterozygous $EXT1^{+/-}$ and $EXT2^{+/-}$ mutant mice did develop multiple osteochondromas by 2 months of age, while companion single heterozygous mice did not as also show previously (Stickens et al., 2005). Because both *EXT1* and *EXT2* are needed for HS synthesis, the compound heterozygous mice were expected to produce about 25% of HS compared to wild-type mice. In this regard, it is interesting to note that a few HME patients have been found to bear germline compound heterozygous mutations in both *EXT1* and *EXT2* (Ishimaru et al., 2016; Jennes et al., 2009; Zuntini et al., 2010). Considering the above, it could be a bold assumption that there is a possiblility of a "second hit" to happen, but the gene of the second hit is highly likely be unmutated in *EXT1*/*EXT2* complex. Compound heterozygous mutations in both *EXT1* and *EXT2* are the most likely cause of the HME. It relates to the more interactions in two genes. Though speculative, we could explain why the expression levels of child HME patients are in line within mice experimental results (heterozygous $EXT1^{+/-}$and $EXT2^{+/-}$ mutant mice). However, it should be noted that this hypothesis remains untested and requires further study.

In addition to pathogenic mechanisms, we have made a lipid testing for this family with HME. We found that HDL and LDL in child HME patients who were in the incidence stage were lower than standard references of normality; however, the measurements in adult HME patients were situated in the normal range. A recent study suggests that genetic variation in heparan sulfate proteoglycans modestly affects postprandial lipid clearance in humans (Mooij et al., 2015). Heparan sulfate proteoglycans (HSPGs) have been identified as coreceptors for PCSK9 on the hepatocyte cell surface to promote PCSK9 uptake and function (Galvan & Chorba, 2019). PCSK9 targets the LDL receptor (LDLR) for degradation and increasing plasma LDL. Following the principle mentioned above, the lower amount (much less than half) of HS synthesis in child HME patients may exist not only in chondrocytes but also of the liver. However, there is no direct evidence for whether this type of situation persists in other humans.

High-throughput next-generation sequencing technologies have been widely utilized in the last ten years, as a growing number of HME patients have an unequivocal genetic diagnosis. There have been considerable advances in this biomedical research. However, most clinical research only focuses on patients and controls. The research about an aging period cohort analysis in a family with HME is scarce. Although we tried to fit our novel assumptions to the available experimental data, further analysis is needed to verify these assumptions. We wondered whether the differences in indicators of child HME patients and adult HME patients is universal among other HME family. We were interested in learning where these occurred "second hit" cells come from. Although most of the studies support that the "second hit" occurs during perichondrium cell division, some studies boldly guess that the additional hit has been

existing in the stem cell phase. While more research will be needed to elucidateapart these and other possibilities, our data do indicate that some indicators between HME children and adults revealed significant differences. Further studies are needed to elucidate potential mechanisms mediating these relationships and should also pave the way for the future development of novel therapeutics for HME and related conditions.

ACKNOWLEDGMENTS

We thank the proband and his family members for their support and participation. This work was supported by a grant from the National Natural Science Foundation of China (General Program Grant No. 82172011).

CONFLICT OF INTEREST

All authors declare that they have no conflict of interest.

AUTHOR CONTRIBUTIONS

JL wrote the manuscript and performed the practical work. ZW collected patient's data. YH, CJ, and DC analyzed the patient's data, who were assisted by ZW. YA-Z designed the study. JZ conceived the study and edited the manuscript.

DATA AVAILABILITY STATEMENT

The data that support the findings of this study are available from the corresponding author upon reasonable request.

ETHICAL COMPLIANCE

This study was approved by the ethics committee of the Second Hospital of Shanxi Medical University.

ORCID

Jianwei Li https://orcid.org/0000-0003-4731-2186
Yaxin Han https://orcid.org/0000-0001-6340-6225
Yong-An Zhou https://orcid.org/0000-0001-5015-7688

REFERENCES

Barash, Y., Calarco, J. A., Gao, W., Pan, Q., Wang, X., Shai, O., Blencowe, B. J., & Frey, B. J. (2010). Deciphering the splicing code. *Nature*, *465*(7294), 53–59. https://doi.org/10.1038/nature09000

Billings, P. C., & Pacifici, M. (2015). Interactions of signaling proteins, growth factors and other proteins with heparan sulfate: mechanisms and mysteries. *Connective Tissue Research*, *56*(4), 272–280. https://doi.org/10.3109/03008207.2015.1045066

Cheng, J., Nguyen, T. Y. D., Cygan, K. J., Celik, M. H., Fairbrother, W. G., Avsec, Z., & Gagneur, J. (2019). MMSplice: modular modeling improves the predictions of genetic variant effects on splicing. *Genome Biology*, *20*(1), 48. https://doi.org/10.1186/s13059-019-1653-z

D'Arienzo, A., Andreani, L., Sacchetti, F., Colangeli, S., & Capanna, R. (2019). Hereditary multiple exostoses: Current insights. *Orthopedic Research and Reviews*, *11*, 199–211. https://doi.org/10.2147/ORR.S183979

Davydov, E. V., Goode, D. L., Sirota, M., Cooper, G. M., Sidow, A., & Batzoglou, S. (2010). Identifying a high fraction of the human genome to be under selective constraint using GERP++. *PLoS Computational Biology*, *6*(12), e1001025. https://doi.org/10.1371/journal.pcbi.1001025

Galvan, A. M., & Chorba, J. S. (2019). Cell-associated heparin-like molecules modulate the ability of LDL to regulate PCSK9 uptake. *Journal of Lipid Research*, *60*(1), 71–84. https://doi.org/10.1194/jlr.M087189

Hecht, J. T., Hayes, E., Haynes, R., Cole, W. G., Long, R. J., Farach-Carson, M. C., & Carson, D. D. (2005). Differentiation-induced loss of heparan sulfate in human exostosis derived chondrocytes. *Differentiation*, *73*(5), 212–221. https://doi.org/10.1111/j.1432-0436.2005.00025.x

Hennekam, R. C. (1991). Hereditary multiple exostoses. *Journal of Medical Genetics*, *28*(4), 262–266. https://doi.org/10.1136/jmg.28.4.262

Huegel, J., Sgariglia, F., Enomoto-Iwamoto, M., Koyama, E., Dormans, J. P., & Pacifici, M. (2013). Heparan sulfate in skeletal development, growth, and pathology: the case of hereditary multiple exostoses. *Developmental Dynamics*, *242*(9), 1021–1032. https://doi.org/10.1002/dvdy.24010

Ishimaru, D., Gotoh, M., Takayama, S., Kosaki, R., Matsumoto, Y., Narimatsu, H., Sato, T., Kimata, K., Akiyama, H., Shimizu, K., & Matsumoto, K. (2016). Large-scale mutational analysis in the EXT1 and EXT2 genes for Japanese patients with multiple osteochondromas. *BMC Genetics*, *17*, 52. https://doi.org/10.1186/s12863-016-0359-4

Jennes, I., Pedrini, E., Zuntini, M., Mordenti, M., Balkassmi, S., Asteggiano, C. G., Casey, B., Bakker, B., Sangiorgi, L., & Wuyts, W. (2009). Multiple osteochondromas: mutation update and description of the multiple osteochondromas mutation database (MOdb). *Human Mutation*, *30*(12), 1620–1627. https://doi.org/10.1002/humu.21123

Jian, X., Boerwinkle, E., & Liu, X. (2014). In silico prediction of splice-altering single nucleotide variants in the human genome. *Nucleic Acids Research*, *42*(22), 13534–13544. https://doi.org/10.1093/nar/gku1206

Jones, K. B., Piombo, V., Searby, C., Kurriger, G., Yang, B., Grabellus, F., Roughley, P. J., Morcuende, J. A., Buckwalter, J. A., Capecchi, M. R., Vortkamp, A., & Sheffield, V. C. (2010). A mouse model of osteochondromagenesis from clonal inactivation of Ext1 in chondrocytes. *Proceedings of the National Academy of Sciences of the United States of America*, *107*(5), 2054–2059. https://doi.org/10.1073/pnas.0910875107

Knudson, A. G., Jr. (1971). Mutation and cancer: Statistical study of retinoblastoma. *Proceedings of the National Academy of Sciences of the United States of America*, *68*(4), 820–823. https://doi.org/10.1073/pnas.68.4.820

Li, P., Zhang, L., Zhao, N., Xiong, Q., Zhou, Y. A., Wu, C., & Xiao, H. (2019). A novel alpha-galactosidase a splicing mutation predisposes to fabry disease. *Frontiers in Genetics*, *10*, 60. https://doi.org/10.3389/fgene.2019.00060

McCormick, C., Duncan, G., Goutsos, K. T., & Tufaro, F. (2000). The putative tumor suppressors EXT1 and EXT2 form a stable complex that accumulates in the Golgi apparatus and catalyzes the synthesis of heparan sulfate. *Proceedings of the National Academy of Sciences of the United States of America*, *97*(2), 668–673. https://doi.org/10.1073/pnas.97.2.668

Mooij, H. L., Bernelot Moens, S. J., Gordts, P. S. M., Stanford, K., Foley, E., van den Boogert, M. W., Witjes, J., Hassing, H. C., Tanck, M., van de Sande, M., Levels, J. H., Kastelein, J. P., Stroes, E. G., Dallinga-Thie, G., Esko, J., & Nieuwdorp, M. (2015). Ext1 heterozygosity causes a modest effect on postprandial lipid clearance in humans. *Journal of Lipid Research*, *56*(3), 665–673. https://doi.org/10.1194/jlr.M053504

Pacifici, M. (2017). Hereditary multiple exostoses: New insights into pathogenesis, clinical complications, and potential treatments. *Current Osteoporosis Reports*, *15*(3), 142–152. https://doi.org/10.1007/s11914-017-0355-2

Quang, D., Chen, Y., & Xie, X. (2015). DANN: A deep learning approach for annotating the pathogenicity of genetic variants. *Bioinformatics*, *31*(5), 761–763. https://doi.org/10.1093/bioinformatics/btu703

Reijnders, C. M., Waaijer, C. J., Hamilton, A., Buddingh, E. P., Dijkstra, S. P., Ham, J., Bakker, E., Szuhai, K., Karperien, M., Hogendoorn, P. C., Stringer, S. E., & Bovée, J. V. (2010). No haploinsufficiency but loss of heterozygosity for EXT in multiple osteochondromas. *The American Journal of Pathology*, *177*(4), 1946–1957. https://doi.org/10.2353/ajpath.2010.100296

Richards, S., Aziz, N., Bale, S., Bick, D., Das, S., Gastier-Foster, J., & ACMG Laboratory Quality Assurance Committee. (2015). Standards and guidelines for the interpretation of sequence variants: a joint consensus recommendation of the American College of Medical Genetics and Genomics and the Association for Molecular Pathology. *Genetics in Medicine: Official Journal of the American College of Medical Genetics*, *17*(5), 405–424. https://doi.org/10.1038/gim.2015.30

Schmale, G. A., Conrad, E. U., 3rd, & Raskind, W. H. (1994). The natural history of hereditary multiple exostoses. *The Journal of Bone and Joint Surgery American*, *76*(7), 986–992. https://doi.org/10.2106/00004623-199407000-00005

Stickens, D., Zak, B. M., Rougier, N., Esko, J. D., & Werb, Z. (2005). Mice deficient in Ext2 lack heparan sulfate and develop exostoses. *Development*, *132*(22), 5055–5068. https://doi.org/10.1242/dev.02088

Wang, G. S., & Cooper, T. A. (2007). Splicing in disease: Disruption of the splicing code and the decoding machinery. *Nature Reviews Genetics*, *8*(10), 749–761. https://doi.org/10.1038/nrg2164

Wells, D., Hill, A., Lin, X., Ahn, J., Brown, N., & Wagner, M. (1997). Identification of novel mutations in the human EXT1 tumor suppressor gene. *Human Genetics*, *99*(5), 612–615. https://doi.org/10.1007/s004390050415

Xiong, H. Y., Alipanahi, B., Lee, L. J., Bretschneider, H., Merico, D., Yuen, R. K., Hua, Y., Gueroussov, S., Najafabadi, H. S., Hughes, T. R., Morris, Q., Barash, Y., Krainer, A. R., Jojic, N., Scherer, S. W., Blencowe, B. J., & Frey, B. J. (2015). RNA splicing. The human splicing code reveals new insights into the genetic determinants of disease. *Science*, *347*(6218), 1254806. https://doi.org/10.1126/science.1254806

Zak, B. M., Schuksz, M., Koyama, E., Mundy, C., Wells, D. E., Yamaguchi, Y., Pacifici, M., & Esko, J. D. (2011). Compound heterozygous loss of Ext1 and Ext2 is sufficient for formation of multiple exostoses in mouse ribs and long bones. *Bone*, *48*(5), 979–987. https://doi.org/10.1016/j.bone.2011.02.001

Zuntini, M., Pedrini, E., Parra, A., Sgariglia, F., Gentile, F. V., Pandolfi, M., Alberghini, M., & Sangiorgi, L. (2010). Genetic models of osteochondroma onset and neoplastic progression: Evidence for mechanisms alternative to EXT genes inactivation. *Oncogene*, *29*(26), 3827–3834. https://doi.org/10.1038/onc.2010.135

How to cite this article: Li, J., Wang, Z., Han, Y., Jin, C., Cheng, D., Zhou, Y-A & Zhen, J. (2022). Genetic and functional analyses detect an *EXT1* splicing pathogenic variant in a Chinese hereditary multiple exostosis (HME) family. *Molecular Genetics & Genomic Medicine*, 10, e1878. https://doi.org/10.1002/mgg3.1878